Journal of Applied Mechanics and Technical Physics, Vol. 44, No. 1, pp. 17–26, 2003

SECONDARY ACOUSTIC WAVES IN A POLYDISPERSE BUBBLY MEDIUM

D. V. Voronin,[1] G. N. Sankin,[1] V. S. Teslenko,[1]
R. Mettin,[2] and W. Lauterborn[2]

UDC 532.529+532.528

Wave interaction of bubbles in a cavitation cluster is studied theoretically and experimentally. It is found that two groups of bubbles with different phases of oscillations and collapse time are formed at the early stage of bubble-cluster formation. It is shown that small bubbles accumulating energy in the initial pulsed acoustic wave collapse in the field of internal positive pressure of the cluster. A secondary compression wave generated by inertial expansion of large bubbles is determined by means of numerical simulation and registered experimentally. The amplitude of this wave is comparable to the amplitude of the initial pulse. A decrease in the oscillation period and strengthening of the microbubble collapse are observed in the cluster under pulsed compression.

Key words*: cavitation, bubbles, shock waves, simulation.*

Introduction. Wave processes in bubbly media have been studied in numerous experimental and theoretical papers [1–3]. Interaction of bubbles in the field of external pulsed waves occurs due to secondary acoustic waves whose propagation pattern is not yet clear. Investigation of wave interaction inside a cavitation bubble cluster has become more important due to research in the multibubble sonoluminescence phenomenon [4].

The collapse of a cavitation bubble is known to involve spherical cumulation of energy [5, 6]. Short flashes of light are observed thereby, and shock waves with intensity depending on bubble dynamics arise [7, 8]. The shape of bubbles in the course of collapse in the field of a shock wave with a plane front is significantly different from spherical [9], and a jet stream is formed inside the bubble.

Subsequent studies of cavitation showed that the cavitation cloud in the course of its formation in a focused acoustic rarefaction wave is a source of a compression wave [10, 11]. A similar effect is observed during the motion of pulsed acoustic waves from a plane source. A single rarefaction wave passing through a bubbly medium may transform into a compression wave [12]. Oscillations of the resultant bubbles give rise to secondary acoustic waves, which interfere and, under certain conditions, generate a powerful secondary compression wave whose amplitude is commensurable with the amplitude of the initial pulse [13, 14].

The effect of collapse intensification due to interaction of bubbles of different sizes was observed by means of mathematical analysis of a bubble cluster in a stationary ultrasonic field [15]. The action of secondary compression waves with an amplitude higher than 10 MPa on microbubbles, which is manifested in cluster luminescence, was studied experimentally in [16]. Here, the collapse of some bubbles occurs in a medium with quasi-isotropically distributed bubbles.

The goal of the present work is to study theoretically and experimentally the dynamics of a cluster of bubbles of different sizes under cavitation and their interaction and to determine conditions of intensification of bubble collapse in the cluster.

Experiment. The layout of the experiment is shown in Fig. 1. Cavitation was induced far from the boundaries of the liquid by an electromagnetic generator of shock waves with a transducer placed on the dish bottom. The transducer was a segment of a sphere with an aperture $D = 70$ mm and a focal length $F = 55$ mm. In the transducer, a low-inductance (less than 5 nH) capacitor (2 μF) is connected to a high-voltage pulsed-charge

[1]Lavrent'ev Institute of Hydrodynamics, Siberian Division, Russian Academy of Sciences, Novosibirsk 630090; [2]Drittes Physikalisches Institut, Universität Göttingen, Göttingen 37073, Germany. Translated from Prikladnaya Mekhanika i Tekhnicheskaya Fizika, Vol. 44, No. 1, pp. 22–32, January–February, 2003. Original article submitted February 11, 2002; revision submitted June 19, 2002.

0021-8944/03/4401-0017 $25.00

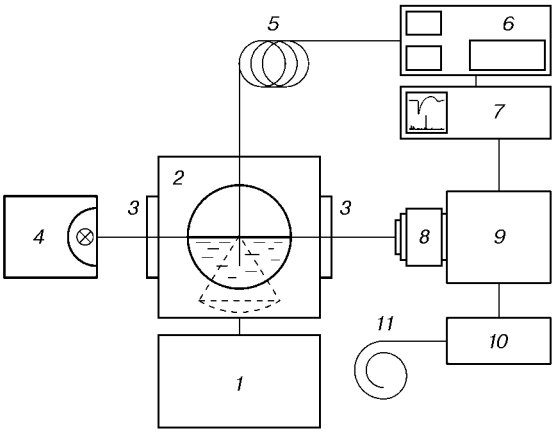

Fig. 1. Layout of the experiment: 1) current-pulse generator; 2) dish; 3) windows; 4) flash lamp; 5) light guide; 6) pressure gauge; 7) oscilloscope; 8) microscope; 9) high-speed camera; 10) delayed-pulse generator; 11) antenna.

device [17]. A discharge of the capacitor forms a powerful current pulse in the coil. Diffusion of the magnetic field through the membrane occurs, and the latter is ejected into the liquid by magnetic pressure. Since the membrane has the form of a spherical segment, a converging pressure pulse is formed in the liquid. The initial pressure p_{m} in the wave near the membrane was set by the voltage on a reservoir capacitor. The dish had two glass windows for photorecording and observation of liquid luminescence. All distances between the focus and dish boundaries were greater than half of the path covered by sound during the observation period. Distilled demineralized water saturated by a gas under conditions of room atmosphere was used. The studies were performed at room temperature. The pressure was measured by an FOPH 300 fiber-optic gauge [18]. The light guide was mounted using micrometric screws. The coordinates of the final position of the light guide were counted from the focal point of the transducer, which was determined by the maximum value of the pressure amplitude for a charge voltage of 5 kV (the z axis coincides with the transducer centerline, and the point with coordinates $z = r = 0$ coincides with its focus). To observe shock-wave propagation and bubble dynamics, we used an IMACON 468 high-speed camera (DRS Hadland LTD, eight frames, exposure time 10 nsec). The required amplification up to 3 μm per pixel was reached by using a QM 100 (Questar) long-focal-length reflection microscope. The object was illuminated from the back side by a powerful xenon lamp (500 J, flash duration 50 μsec). The flash was located at a large distance (more than 1 m) from the dish, so that the light beam reflected by the mirror was weakly divergent. The use of this layout allowed us to observe both the cavitation bubbles and the shock fronts generating refractive index gradients. The signals were recorded by a TDS 784A digital oscilloscope (Tektronix, analog input 1 GHz). The oscilloscope and the camera were triggered by the delayed-pulse generator from the pickup on the antenna caused by the generator discharge. The time Δt was counted from the moment of compression-wave arrival at the observation point.

As was shown previously (see, e.g., [19]), the development of the cavitation cloud occurs in a converging wave consisting of a compression phase and a subsequent expansion phase. The cavitation zone is an ellipsoid of revolution (with an axial length of 15 mm and cross-sectional diameter of 6 mm). This is caused by the fact that the zone of distribution of the negative pressure peak is also shaped as an ellipsoid of revolution.

By means of photorecording, we measured the coordinates of the center and the bubble diameter in the cluster (Fig. 2). The point O in Fig. 2 has the coordinates $z = -4.5$ mm and $r = 0$. Figure 3 shows the bubble diameter versus the time Δt. Statistical processing of data in the interval $\Delta t = 3$–4 μsec revealed two groups of bubbles: growing bubbles (I) and collapsing bubbles (II). It was found that the period of bubble oscillations depends on the time needed for the nucleus to reach registrable dimensions. It follows from Fig. 3 that bubbles of the first and second groups become registrable in 1.6 and 2.1 μsec, respectively, after arrival of the compression-wave front. Bubbles of the second group collapse at times within the interval of 3.5–4.5 μsec on the background of growth of large bubbles. After the first collapse, bubbles of the second group expand with their spherical shape preserved. The distribution of bubbles of the second group along the coordinate r has a width of 1.2 mm at the half-height. The distribution of bubbles of both groups along the z axis is uniform. After the time mentioned, expansion of bubbles of both groups is observed, and they increase approximately to identical dimensions.

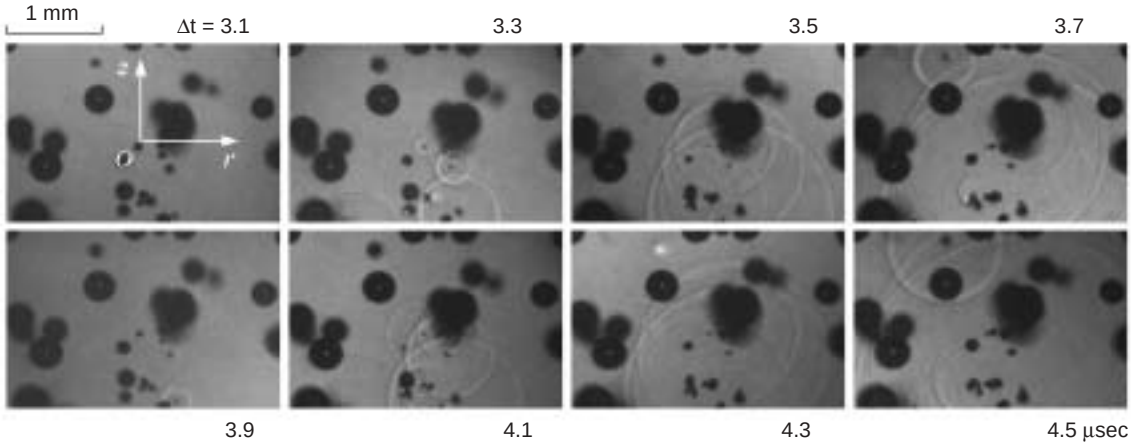

Fig. 2. Frames of high-speed microscopic photorecording of the central region of the cluster.

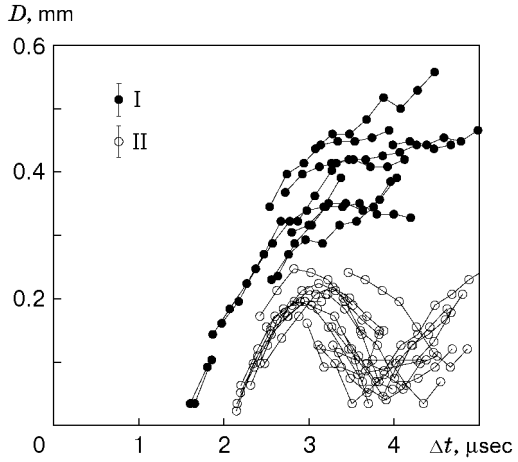

Fig. 3. Bubble diameter at the center of the cluster versus time: points I and II refer to bubbles of the first and second groups, respectively.

The pressure was measured in the region outside the cavitation cloud. Figure 4 shows the pressure profiles for $p_{\rm m} = 4.3$ (without developed cavitation) and 5.9 MPa (with developed cavitation) in the focus $r = 0$, $z = 0$. For $p_{\rm m} = 5.9$ MPa, an additional pressure peak with a positive-phase amplitude up to 10 MPa, which directly followed the rarefaction wave, was observed within the time interval $\Delta t = 2.5$–2.8 μsec (Fig. 4b). The negative component of the signal ahead of the shock-wave front near the focus ($|z| \leqslant 5$ mm) is caused by reflection of the probing beam of the gauge from the shock-wave front[1] and can be reduced to zero by turning of the optical fiber by an angle greater than 30°. The pressure profile in Fig. 4a (rise time, length and amplitude of compression and rarefaction pulses) is similar to the pressure profile measured in the absence of cavitation [18]. In our case, the amplitude of waves produced by collapsing bubbles (see Fig. 2) considered in detail in [20, 21] was below the sensitivity threshold of the gauge.

An analysis of numerical results shows that the reason for such a behavior of small bubbles is the influence of large bubbles located nearby. Expanding simultaneously due to inertia acquired in the initial wave, the bubbles displace the liquid from the interbubble space, re-radiating sonic energy in the form of a spherical wave. Interference of waves scattered on individual bubbles results in the formation of a high-pressure pulse immediately behind the expansion phase of the initial wave (Fig. 4b); this pulse diverges from the cavitation cloud in a cone whose centerline coincides with the transducer axis. The pressure in the liquid cavitating behind the wave acquires an oscillating character, which was first observed in [11, 12] and is confirmed by the calculation results presented below.

[1]Private communication of W. Eisenmenger.

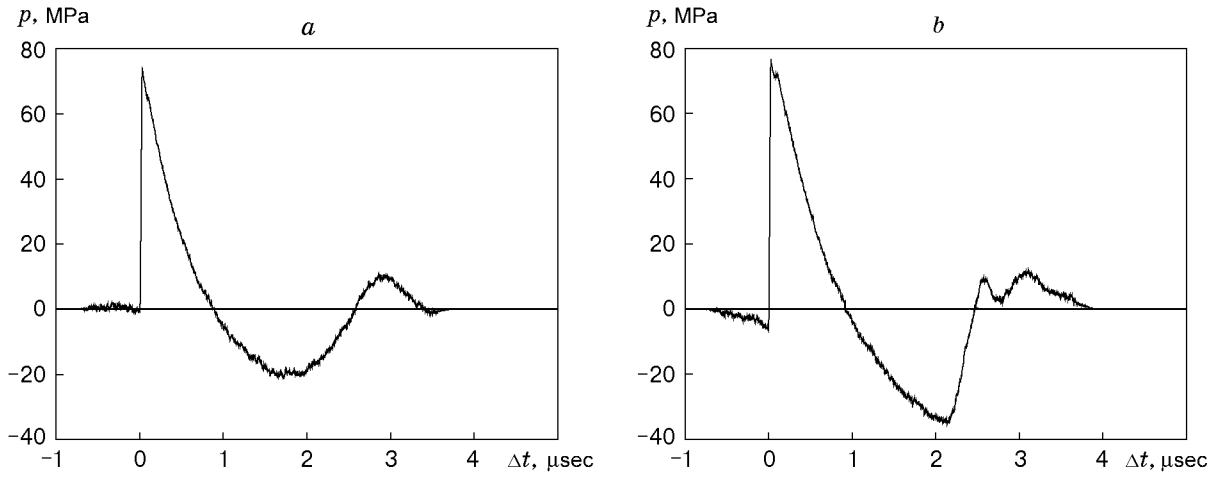

Fig. 4. Pressure in the focus $z = r = 0$ as a function of Δt for $p_{\rm m} = 4.3$ (a) and 5.9 MPa (b).

Mathematical Simulation. The experimental data show that bubbles may have a significantly different behavior when an acoustic wave passes through a cavitating liquid. Two groups of bubbles with a substantially different time of the first collapse can be identified. To find the reason for this difference and to study the formation mechanism of secondary waves and the character of bubble interaction, we modeled the motion of an initiating pulse through a single bubble or a set of bubbles of different diameters located at a certain distance from each other.

We consider the flow in a vertically located circular tube filled by water with an initial pressure $p_0 = 0.1$ MPa. Gas bubbles with the same pressure were placed into the tube center. The system "liquid–gas bubbles" was initially in the state of static equilibrium, and the medium velocity was equal to zero. The pulse was initiated at the lower closed end of the tube; it was a plane sinusoidal wave consisting of compression and rarefaction phases. The length of each phase was 5 mm, and the wave amplitude was ± 11.5 MPa. There is a delay of wave arrival between the compression and rarefaction phases; in most cases, it equals 2 mm. The pulse character is in agreement with the above-cited experimental data. In a certain time, the pressure pulse passes through the bubbles, and the system acquires a significantly nonequilibrium character with the formation of secondary waves. For a detailed study of the formation mechanism and interaction of waves, the initiating pulse was considered in some calculations either as the rarefaction phase or the compression phase only. It was assumed that the side walls of the tube are closed (solid walls), and the upper end is open.

The pulse character, the initial position of the bubbles, and the boundary conditions allow us to assume that the flow is axially symmetric (the axis of symmetry is the tube centerline). The origin of the coordinate system is located on the axis of symmetry at the lower end of the tube. The z axis (along the tube centerline) coincides with the initiating pulse direction, and the r axis is normal to the z axis.

The flow of a two-phase compressible medium "liquid–gas bubbles" is described by unsteady two-dimensional equations of conservation of mass, momentum, and energy with no allowance for diffusion effects:

$$\frac{\partial \bar\sigma}{\partial t} + \frac{\partial \bar a}{\partial z} + \frac{\partial \bar b}{\partial r} = -\frac{1}{r}\,\bar f,$$

$$\bar\sigma = (\rho, \rho u, \rho v, \rho E), \qquad \bar a = (\rho u, \rho u^2 + p, \rho uv, u(\rho E + p)), \tag{1}$$

$$\bar b = (\rho v, \rho uv, \rho v^2 + p, v(\rho E + p)), \qquad \bar f = (\rho v, \rho uv, \rho v^2, v(\rho E + p)).$$

Here ρ is the density, u and v are the velocity-vector components in the z and r directions, respectively, E is the total energy per unit mass, and p is the pressure.

The lower boundary of the computational domain is the tube centerline. The no-penetration condition is imposed on the lateral ($v = 0$) and lower ($u = 0$) boundaries. The boundary conditions at the upper end of the tube correspond to conditions on the free surface.

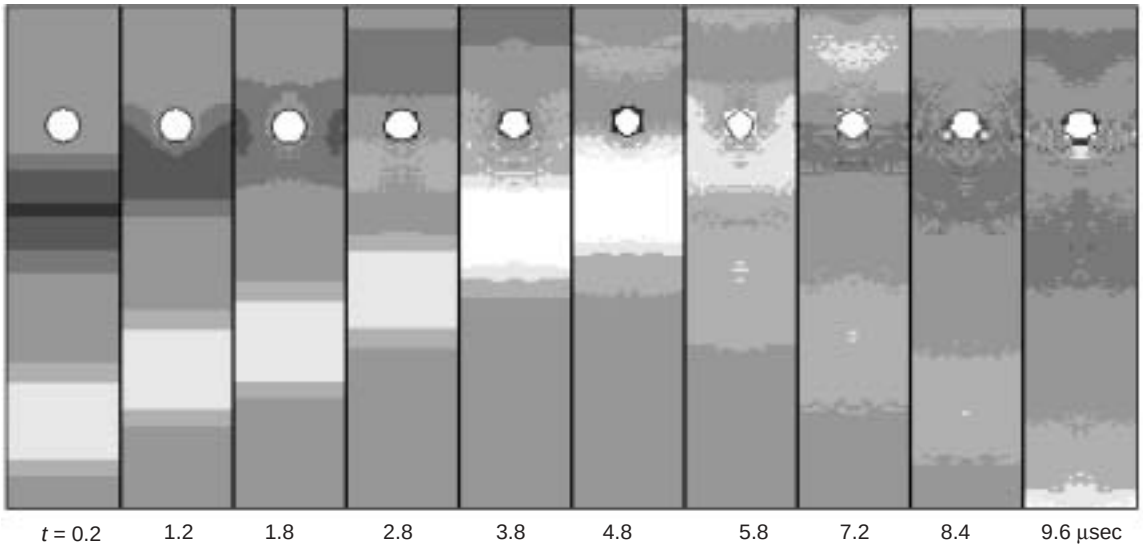

Fig. 5. Sequence of frames for a single bubble in an acoustic wave.

We assume that the gas in the bubble completely satisfies the equation of state of an ideal gas. Then, the closing relations for system (1) in the gas phase are

$$E = E_{\text{in}} + (u^2 + v^2)/2, \qquad E_{\text{in}} = p/((\gamma - 1)\rho),$$

where E_{in} is the internal energy per unit mass and γ is the ratio of specific heats.

The flow in the liquid is described by the first three equations of system (1) (without the law of conservation of energy). To close the system, we used the relations [22] that determine the shock adiabat for water

$$D = C + LU, \qquad \rho(D - U) = \rho_0 D,$$

$$p = \rho_0 DU + p_0, \qquad E = (p + p_0)(1/\rho_0 - 1/\rho)/2 + E_0,$$

where D is the shock-wave velocity, U is the mass velocity behind the shock-wave front, and L and C are constants; the subscript 0 refers to the initial state.

The problem was solved numerically using the method of individual particles developed in [23]. A similar problem for a single bubble with a chemically active gas was solved in [24]. In the present work, particular attention was paid to the mutual influence of the bubbles. Unsteady fields of the basic thermodynamic parameters were calculated both inside each bubble and in the external liquid flow. It was assumed that the liquid–bubble interface is a contact discontinuity with identical pressures on both sides of the discontinuity and a continuous normal-to-discontinuity component of the velocity vector of the medium. In the course of time, the gas bubble could deform, split into several bubbles, or coalesce with other bubbles.

Calculation Results. The following values of parameters were used in calculations: $\rho_{01} = 1$ g/cm^3, $C = 1.7$ km/sec, and $L = 1.7$ for the liquid and $\rho_{02} = 1.225 \cdot 10^{-3}$ g/cm^3 and $\gamma = 1.4$ for air. The size of the computational domain was $z \times r = 35 \times 4$ mm.

Figure 5 shows the calculated sequence of frames of pressure-pulse propagation in water with a single gas bubble. The initial bubble radius was $R_0 = 0.5$ mm; the coordinates of the bubble center were $z_0 = 12.8$ mm and $r_0 = 0$. The dark and light colors in the frames refer to compression and rarefaction waves; the wave amplitude is indicated by various shades of gray. The time is counted from the beginning of pulse motion from the lower end of the tube. The compression wave reaches the bubble at $t = 0.4$ μsec and leaves the vicinity of the bubble at $t = 2.5$ μsec. The bubble starts to shrink in the compression wave; due to inertia, this process continues behind the latter. The compression phases lasts by the time $t = 5$ μsec; the bubble volume decreases approximately twofold. The compression wave loses a significant part of its energy in the flow around the bubble; its amplitude at $t = 2.8$ μsec and later is about 4 MPa. Part of the wave energy is accumulated by the bubble during its compression. In addition, a secondary rarefaction wave is formed due to reflection from the liquid–gas interface, which is clearly seen under the bubble in frame 4 of Fig. 5. At $t = 4.6$ μsec, the rarefaction phase of the initial pulse reaches the

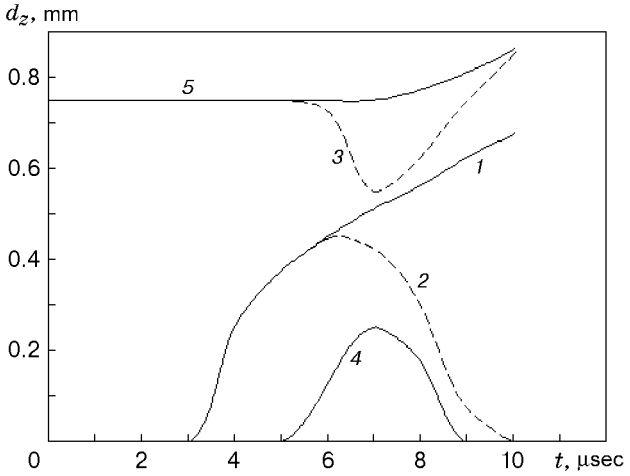

Fig. 6. Variation of the longitudinal size of the bubbles d_z in rarefaction waves: 1) single nucleus; 2, 3) nucleus and large bubble for the wave passing first through the nucleus; 4, 5) nucleus and large bubble for the wave passing first through the large bubble.

bubble. Its reflection from the free surface and the started process of bubble expansion lead to the formation of a secondary compression wave. By the time $t = 9.6$ μsec, a complex consisting of the initiating pulse and secondary compression wave, whose intensities are comparable, and moving toward the open end of the tube is formed. As the initial bubble radius decreases, the pattern remains qualitatively the same [13, 14]. In this case, the processes of reflection from the interface are less important and the minimum size of collapsing bubbles decreases, which increases the amplitude of the secondary compression wave and decreases its length. As is seen in frames 8–10 in Fig. 5, the bubble surface is unstable under the transient pulse, and toroidal waves are formed. The character of these waves is irregular due to the significantly unsteady external flow caused, in particular, by the influence of the tube walls. The center of mass of the bubble is not substantially displaced during the time mentioned.

It follows from the above information that the internal energy of the gas bubble increases in the initial phase of compression, and the secondary wave is formed during the rapid decrease in pressure in the vicinity of the gas bubble. Therefore, to study the formation mechanism of secondary waves, it seems reasonable to study the motion of a single rarefaction wave in the liquid and the corresponding process of expansion of the microbubble to visible dimensions.

The calculated results for several variants of the behavior of the longitudinal size of the bubble in rarefaction waves are shown in Fig. 6.

The data plotted in Fig. 7 refer to propagation of a rarefaction wave of the same amplitude and length as in the above calculations. The center of a microbubble of radius equal to 10 μm is located at a point with coordinates $z = 7.5$ mm and $r = 0$. The microbubble is initially in the state of dynamic equilibrium with the liquid at $p_0 = 0.1$ MPa (it cannot be seen in the first frame of Fig. 7 because of the small size). The bubble nucleus starts to expand in the rarefaction wave, generating a secondary compression wave close to spherical and clearly visible, for instance, in frame 5. Because of the instability of the liquid–gas interface, a wave that shapes the liquid into a jet is formed on the bubble surface (frames 8 and 9). By the time $t = 10$ μsec, the mean radius of the bubble is greater than 300 μm. The variation of the longitudinal size of the bubble d_z in time is shown by curve 1 in Fig. 6.

We consider the process of bubble origination in a liquid with rather large bubbles already existing there. The simulation results are shown in Fig. 8. The initial parameters of the incident wave and microbubble are the same as in the previous case. The bubble center is located at the point $z = 7$ mm and $r = 0$. At the point $z = 10.35$ mm and $r = 0$, there is the center of another bubble of radius 0.35 mm, which is also in dynamic equilibrium. At the first stages, the process of microbubble expansion proceeds in the same manner as in Fig. 7. The bubble becomes visible by the time $t = 3.5$ μsec; a compression wave starts to form in the vicinity of the large bubble at the same time. The expanding first bubble generates a secondary rarefaction wave, which reaches the vicinity of the second bubble by the time $t = 6$ μsec and deforms the latter (curve 3 in Fig. 6). The microbubble reaches the maximum size by the time $t = 6.4$ μsec (curve 2 in Fig. 6), and its radius becomes comparable to the current radius of the

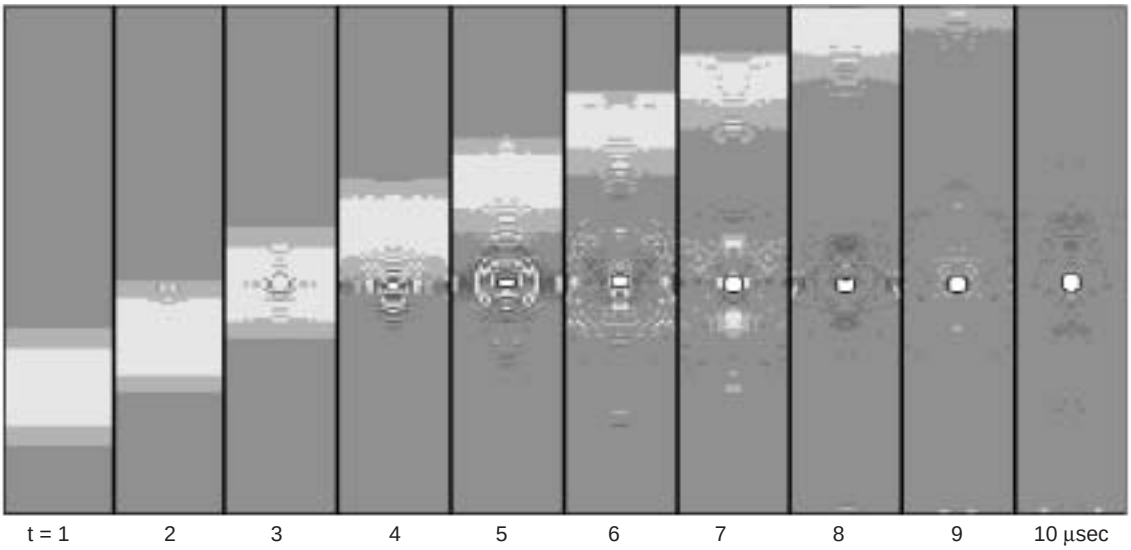

Fig. 7. Origination of a single bubble in a rarefaction wave.

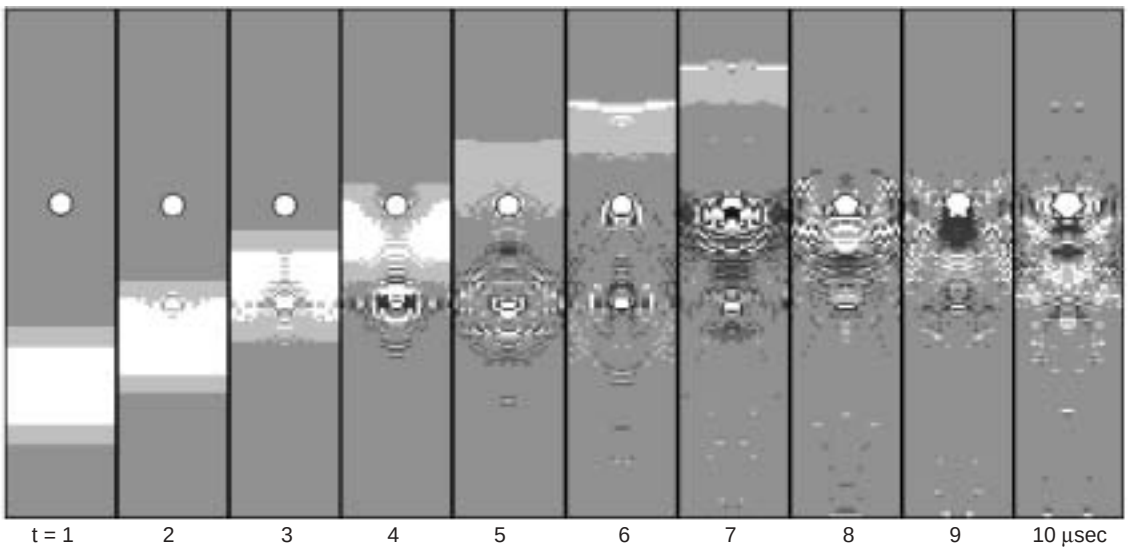

Fig. 8. Mutual influence of bubbles of different diameters in a rarefaction wave.

large bubble. A powerful compression wave formed due to interaction of two secondary waves starts to move in the opposite direction, toward the smaller bubble. The length of this wave is rather large, since its generation is supported by the expanding large bubble. This results in collapsing of the first bubble, and it becomes invisible by the time $t = 10$ μsec. Later on, the amplitude of its second oscillation reaches the amplitude of the first oscillation, and subsequent oscillations gradually decay. The amplitudes of secondary waves in the vicinity of the bubbles are higher than the amplitude of the initiating rarefaction wave. Since the pressure in the diagrams is normalized to the maximum pressure in the channel, the initial wave is invisible in Fig. 8 beginning from frame 8. Though the current sizes of the bubbles may be comparable at some times ($t = 6$–7 μsec), the above-described process is significantly different from that shown in Fig. 7, namely, the period of the first oscillation of the microbubble is considerably smaller.

Figure 9 shows the calculation results for the opposite positions of the bubbles. The initial sizes and the distance between the bubbles correspond to the previous case. The rarefaction wave first passes through the large bubble and then moves toward the nucleus of the small bubble. A visible bubble arises in the cavitation region of the large bubble at $t > 5$ μsec, reaches the maximum radius of 115 μm at $t = 7.2$ μsec, and starts to collapse, since

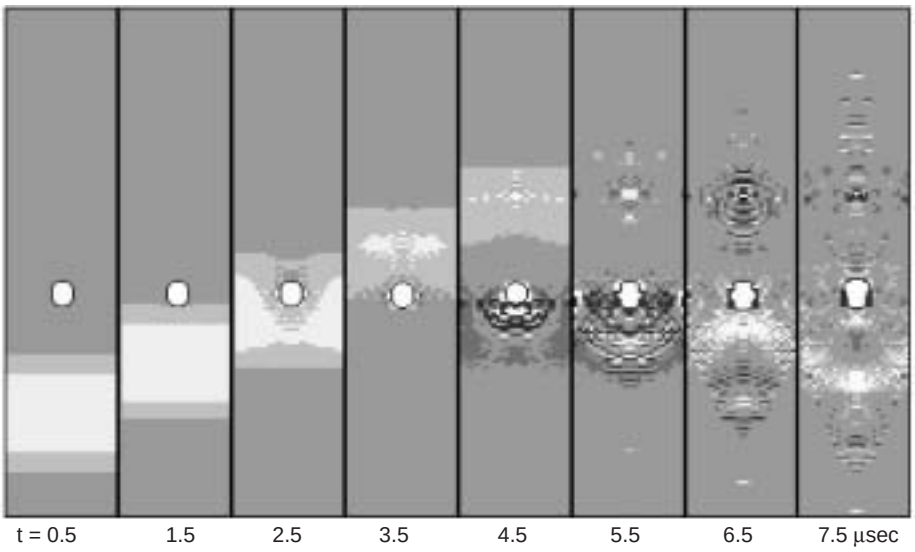

Fig. 9. Origination of a small bubble in the region of acoustic influence of a large bubble.

the secondary compression wave moving from the large bubble behind the initiating rarefaction wave suppresses the expansion process (curve 4 in Fig. 6). In contrast to the previous case, the longitudinal size of the large bubble at the times mentioned increases monotonically in the rarefaction wave (curve 5 in Fig. 6). It should be noted that compression waves arising in the vicinity of the large bubble have different amplitudes. The wave moving downward is more intense, since the amplitude of the initiating rarefaction wave decreases in the flow around the bubble.

It follows from Fig. 6 that the expansion phase of the large bubble (curves 3 and 5) coincides with the collapse phase of the small bubble (curves 2 and 4), independent of their positions. If the small bubble is located behind the large bubble, its maximum size is significantly smaller than in the opposite initial position. The results of mathematical simulation presented here are in agreement with the experimental results plotted in Fig. 3. In particular, the period of the first oscillation of the small bubble coincides with the experimental value and equals 2–4 μsec.

Thus, the calculation results show that energy redistribution occurs in a liquid with bubbles of different diameters. Being able to reach rather large dimensions at some initial period of time, small bubbles collapse under the action of pressure waves from large bubbles.

Similar results were obtained for a pressure pulse consisting of compression and rarefaction phases. The difference from the results in Figs. 7–9 is the fact that the pressure in the bubbles by the moment of rarefaction-wave arrival is significantly higher than the pressure in the ambient liquid, and the amplitude of secondary compression waves is higher in this case.

Conclusions. Thus, it was found that the dynamics of bubbles in a cluster formed by transient pulsed waves in a liquid significantly depends on initial conditions. If the neighboring bubbles in dynamic equilibrium have different radii at a certain time, a pulsed acoustic action (under certain conditions) leads to a collapse of small bubbles with simultaneous expansion of large bubbles.

The bubble dynamics in the cluster is determined by acoustic waves from the neighboring bubbles. An analysis of results of a numerical experiments for a polydisperse medium revealed the formation mechanism of a pulse of positive internal pressure in the cluster, which was experimentally registered as a compression phase following the rarefaction phase of the initial wave (see Fig. 4). An analysis of dynamics of the bubble size in the rarefaction wave for different initial dimensions and relative positions of the bubbles (see Fig. 6) revealed the coincidence of the beginning of the expansion phase of the large bubble and the collapse phase of the small bubble, independent of their relative positions. If the small bubble is located behind the large bubble (with respect to the propagation direction of the initial wave), then its maximum size is significantly smaller than in the case of the opposite initial position. Hence, the relative positions of the bubbles in a polydisperse cluster is the governing factor of formation of secondary acoustic waves.

The calculation results show that energy redistribution occurs in a medium with bubbles of two different initial radii. During expansion, the small bubble transfers its energy to the large bubble, then its growth becomes less intense, and the small bubble collapses under the action of a secondary compression wave induced by the large bubble. This allows us to explain the experimentally observed collapse of some bubbles, whereas other bubbles remain visible.

The results of mathematical simulation are in agreement with experimental data (see Fig. 3). In particular, the period of the first oscillation of the small bubble coincides with the experimental value and equals 2–4 μsec. The collapse time of small bubbles is one order of magnitude smaller than the collapse time of bubbles of the same maximum diameter at atmospheric pressure.

This work was supported by the Russian Foundation for Fundamental Research (Grant Nos. 00-02-17992, 01-02-06444-mas, and 02-02-06838-mas) and German Academic Exchange Service (Grant No. A/00/01480).

REFERENCES

1. S. S. Kutateladze and V. E. Nakoryakov, *Heat and Mass Transfer and Waves in Gas–Liquid Systems* [in Russian], Nauka, Novosibirsk (1984).
2. R. I. Nigmatulin, *Dynamics of Multiphase Media*, Part 1, Hemisphere, New York (1991).
3. V. K. Kedrinskii, *Explosion Hydrodynamics: Experiment and Models* [in Russian], Izd. Sib. Otd. Ross. Akad. Nauk, Novosibirsk (2000).
4. M. A. Margulis, "Sonoluminescence," *Usp. Fiz. Nauk*, **170**, No. 3, 263–287 (2000).
5. E. I. Zababakhin and I. E. Zababakhin, *Phenomena of Unlimited Cumulation* [in Russian], Nauka, Moscow (1988).
6. V. S. Teslenko, "Experimental investigations of the kinetic energy singularities of a collapsing bubble from laser breakdown in a viscous liquid," *J. Appl. Mech. Tech. Phys.*, **17**, No. 4, 543–549 (1976).
7. V. S. Teslenko, "Experimental investigation of bubble collapse at laser-induced breakdown in liquids," in: *Cavitation and Inhomogeneities in Underwater Acoustics*, Proc. of the 1st Int. Conf. (Göttingen, Germany, July 9–11, 1979), Springer-Verlag, Berlin–Heidelberg–New York (1980), pp. 30–34.
8. C. D. Ohl, O. Lindau, and W. Lauterborn, "Luminescence from spherically and aspherically collapsing laser induced bubbles," *Phys. Rev. Lett.*, **80**, 393–396 (1998).
9. J. P. Dear, J. E. Field, and A. J. Walton, "Gas compression and jet formation in cavities collapsed by a shock wave," *Nature*, **332**, 505–508 (1988).
10. V. S. Teslenko, "Shock-acoustic breakdown in a liquid. Kinetics of forced acoustic scattering in focusing of shock waves," *Pis'ma Zh. Tekh. Fiz.*, **20**, No. 5, 51–56 (1994).
11. V. S. Teslenko, "Transformation of rarefaction waves into shock waves under focused shocks in a liquid," in: *Proc. of the 20th Int. Symp. on Shock Waves* (ISSW-20) (Pasadena, U.S.A., July 23–28, 1995), Cal. Inst. of Technol., Pasadena (1995), pp. 511–512.
12. V. K. Kedrinskii, V. A. Vshivkov, G. I. Dudnikova, and Yu. I. Shokin, "Wave interaction in chemically active bubbly media," *Dokl. Ross. Akad. Nauk*, **349**, No. 2, 185–188 (1996).
13. D. V. Voronin, G. N. Sankin, and V. S. Teslenko, "Modeling of secondary compression waves under conditions of cavitation," in: *Physical Acoustics, Propagation, and Diffraction of Waves* (collected scientific papaes of XI Session of the Russian Acoustic Society) [in Russian], Vol. 1, GEOS, Moscow (2001), pp. 175–179.
14. V. D. Voronin, V. S. Teslenko, and G. N. Sankin, "The rarefaction wave transformation into compression wave in a cavitating liquid," in: *Progress in Nonlinear Science*, Proc. Int. Conf. Dedicated to the 100th Anniversary of A. A. Andronov (Nizhny Novgorod, July 2–6, 2001), Univ. of Nizhny Novgorod, Nizhny Novgorod (2001), pp. 334–335.
15. R. I. Nigmatulin, I. Sh. Akhatov, N. K. Vakhitova, et al., "Mathematical modeling of a single bubble and multibubble dynamics in a liquid," in: *Dynamics of Multiphase Systems*, Proc. of the Int. Conf. on Multiphase Systems, Gilem Publ., Ufa (2000), pp. 294–301.
16. G. Sankin, R. Mettin, R. Geisler, et al., "Early stage of bubble dynamics and luminescence in water in a converging shock reflected by a free surface," in: O. von Estorff (ed.), *Fortschritte der Akustik*, Proc. of the DAGA-2001 Conf. (Oldenburg), S. n., Hamburg (2001), pp. 258–259.
17. V. V. Mitrofanov, V. S. Teslenko, V. A. Maier, and A. I. Kudryashov, "Preliminary studies of shock-wave focusing in water for objectives of contactless lithoclasty and therapy of human internal," Report No. 43/89, Inst. Hydrodynamics, Sib. Div., USSR Acad. Sci., Novosibirsk (1990).

18. J. Staudenraus and W. Eisenmenger, "Fibre-optic probe hydrophone for ultrasonic and shock wave measurement in water," Ultrasonics, **31**, 267–273 (1993).
19. G. N. Sankin, R. Mettin, W. Lauterborn, and V. S. Teslenko, "Secondary acoustic waves under conditions of shock-wave cavitation," in: *Physical Acoustics, Propagation, and Diffraction of Waves* (collected scientific papaes of XI Session of the Russian Acoustic Society) [in Russian], Vol. 1, GEOS, Moscow (2001), pp. 32–35.
20. V. K. Kedrinskii, "Propagation of perturbations in a liquid containing gas bubbles," *J. Appl. Mech. Tech. Phys.*, **9**, No. 4, 370–376 (1968).
21. V. E. Nakoryakov, B. G. Pokusaev, and I. R. Shreiber, *Wave Propagation in Gas– and Vapor–Liquid Media* [in Russian], Inst. Thermal Physics, Sib. Div., USSR Acad. Sci., Novosibirsk (1983).
22. R. F. Trunin, "Compression of condensed substances by high pressures of shock waves (laboratory studies)," *Usp. Fiz. Nauk*, **171**, No. 4, 387–414 (2001).
23. V. A. Agureikin and B. P. Kryukov, "Method of individual particles for calculating flows of multispecies media with high strains," in: *Numerical Methods of Mechanics of Continuous Media* (collected scientific papers) [in Russian], Vol. 17, No. 1, Novosibirsk (1986), pp. 17–31.
24. F. N. Zamaraev, V. K. Kedrinskii, and C. Mader, "Waves in a chemically active bubble medium," *J. Appl. Mech. Tech. Phys.*, **31**, No. 2, 179–184 (1990).